

Evaluation of the Performance of CFSR Reanalysis Data Set for Estimating Potential Evapotranspiration (PET) in Turkey

AHMET IRVEM (✉ airvem@mku.edu.tr)

Hatay Mustafa Kemal Üniversitesi: Hatay Mustafa Kemal Üniversitesi <https://orcid.org/0000-0002-3838-1924>

Mustafa OZBULDU

Hatay Mustafa Kemal Üniversitesi: Hatay Mustafa Kemal Üniversitesi

Research Article

Keywords: CFSR re-analysis, Potential evapotranspiration, FAO56-PM, Turkey

Posted Date: November 23rd, 2021

DOI: <https://doi.org/10.21203/rs.3.rs-977416/v1>

License:  This work is licensed under a Creative Commons Attribution 4.0 International License.

[Read Full License](#)

Evaluation of the performance of CFSR reanalysis data set for estimating potential evapotranspiration (PET) in Turkey

Ahmet IRVEM^{1*}, Mustafa OZBULDU¹

¹Department of Biosystems Engineering, Faculty of Agriculture, Hatay Mustafa Kemal University, 31040, Antakya, Hatay, Turkey.

*Corresponding Author: Dr. Ahmet IRVEM e-mail: airvem@mku.edu.tr

Abstract

Evapotranspiration is an important parameter for hydrological, meteorological and agricultural studies. However, the calculation of actual evapotranspiration is very challenging and costly. Therefore, Potential Evapotranspiration (PET) is typically calculated using meteorological data to calculate actual evapotranspiration. However, it is very difficult to get complete and accurate data from meteorology stations in, rural and mountainous regions. This study examined the availability of the Climate Forecast System Reanalysis (CFSR) reanalysis data set as an alternative to meteorological observation stations in the computation of potential annual and seasonal evapotranspiration. The PET calculations using the CFSR reanalysis dataset for the period 1987-2017 were compared to data observed at 259 weather stations observed in Turkey. As a result of the assessments, it was determined that the seasons in which the CFSR reanalysis data set had the best prediction performance were the winter ($C' = 0.76$ and $PBias = -3.77$) and the autumn ($C' = 0.75$ and $PBias = -12.10$). The worst performance was observed for the summer season. The performance of the annual prediction was determined as $C' = 0.60$ and $PBias = -15.27$. These findings indicate that the results of the PET calculation using the CFSR reanalysis data set are relatively successful for the study area. However, the data should be evaluated with observation data before being used especially in the summer models.

Keywords: CFSR re-analysis, Potential evapotranspiration, FAO56-PM, Turkey.

1. Introduction

The amount of water that evaporates from soil surfaces or open water and the transpiration of plant leaves in the atmosphere is known as evapotranspiration (Tabari et al. 2013; Anderson et al. 2019). Evapotranspiration for hydrological, meteorological, and agricultural studies is a parameter that

28 plays an important role in the planning of water resources, programming of irrigation time, and the
29 creation of hydrological and agricultural models. Evapotranspiration; lysimeter (Gebler et al. 2015),
30 Eddy-covariance method (Sun et al. 2008), Bowen ratio energy balance (Shi et al. 2008),
31 scintillometer (Moorhead et al. 2017) and evaporation pans (Conceicao 2002) can be measured.
32 However, these procedures are quite costly and difficult to apply in large basin conditions (Latrech et
33 al. 2019).

34 Potential evapotranspiration is defined as the amount of water that can evaporate when the
35 water in the soil is sufficient to meet the atmospheric moisture demand (Allen et al. 1998). The PET is
36 extremely useful to measure the atmospheric water demand of the area. Therefore, it is used in a
37 variety of applications, including irrigation planning, drought monitoring and understanding the
38 impacts of climate change (Lang et al. 2017).

39 Numerous methodologies have been developed to determine potential evapotranspiration
40 (PET) and actual evapotranspiration using meteorological data (Bandyopadhyay et al. 2012). These
41 methods are mostly based on solar radiation (Priestley Taylor), temperature (Thornthwaite,
42 Hargreaves, and Samani), and a combination of solar radiation and temperature (Penman-Monteith)
43 (Seong et al. 2017; Purnadurga et al. 2019). The FAO56-PM method is considered a good way to
44 estimate evapotranspiration globally, compared to other methods. (Sentelhas et al. 2010; Srivastava et
45 al. 2013; Tabari et al. 2013; Tanguy et al. 2018).

46 Kite and Drooger (2000) assessed eight different PET calculation methods and explained that
47 the FAO56-PM method is most compatible with field observations. The FAO56-PM is a combination
48 of physiological and aerodynamic methods that require climate factors like maximum and minimum
49 temperature, wind speed, relative humidity and solar radiation. However, the meteorological stations
50 providing these data, particularly in developing countries, are not distributed uniformly (Alfaro et al.
51 2020). In addition, observations of these climatic variables are very difficult to obtain in rural and
52 mountainous areas. In addition, setting up and maintaining the meteorological station at these
53 locations is quite costly (Tabari et al. 2013; Lang et al. 2017). Therefore, alternative data sources are
54 needed to better simulate hydrological processes. Therefore, additional data sources such as the
55 reanalysis data set are necessary to better simulate hydrological processes. Reanalysis datasets with

56 high precision and high spatiotemporal resolution widely use in hydrological modelling (Alfaro et al.
57 2020).

58 Re-analysis data sets are generated using data from meteorology observation stations based on
59 satellite data, weather forecast models, and data assimilation methods (Purnadurga et al. 2019). There
60 are many commonly used re-analysis data sets. These are CFSR (Saha et al. 2010), NCEP/DOE
61 (Kanamitsu et al. 2002), and NCEP/NCAR (Kalnay et al. 1996) datasets produced by NCEP, ERA-15
62 (Bromwich et al. 2005), ERA40 (Uppala et al. 2005) and ERA-Interim (Dee et al. 2011) datasets
63 produced by ECMWF, JRA-55 (Ebita et al. 2011) datasets from Japanese meteorology agency and
64 MERRA (Rienecker et al. 2011) datasets by NASA.

65 These datasets provide predictions of weather variables, including precipitation and
66 temperature, for any terrestrial location around the world. The NCEP-CFSR re-analysis dataset uses
67 numerical weather prediction techniques to predict atmospheric conditions with a resolution of 0.3125
68 (~ 38 km). In addition, forecasting models are restarted every 6 hours using information from the
69 global network of weather stations (Fuka et al. 2013). The most important advantage of CFSR is that it
70 provides complete and continuous recording of climate data such as precipitation, temperature, solar
71 radiation, humidity, and wind speed since 1979 (Auerbach et al. 2016). In addition, the complete
72 acquisition of these data allows the use of the FAO56-PM method.

73 Laurie et al. (2014) evaluated, reanalysis data for the Mekong basin as input to the
74 hydrological model. They indicated that if there is a lack of data, CFSR temperature data can be used
75 for hydrological modelling studies. Fuka et al. (2013) investigated the usability of the CFSR data set
76 as historical weather data in modeling five basins with hydrological different climate regimes. As a
77 result, they explained that the modeling made with CFSR temperature and precipitation data gives
78 results as well as the modeling using observation and measurement stations, and they reported that the
79 CFSR data set can be used in basins without observation and measurement stations. Dial and
80 Srinivasan (2014) assessed whether or not the CFSR dataset is appropriate for hydrologic modeling.
81 As a result of the evaluations, they explained that the CFSR data set is an important alternative for
82 hydrological estimates in areas where observation data are not available. In other studies, Alemayehu
83 et al. (2015) evaluated the ability to calculate potential evapotranspiration with sufficient accuracy,

84 using different reanalysis datasets. They compared the PET estimates calculated using the CFSR
85 dataset with the results of the observation stations and reported that the CFSR dataset is a good
86 alternative. Alfaro et al. (2020) calculated the potential evapotranspiration required for hydrological
87 modeling with the CFSR reanalysis data set in their study. They explained that the predictive
88 performance of the CFSR dataset was good by evaluating the results obtained.

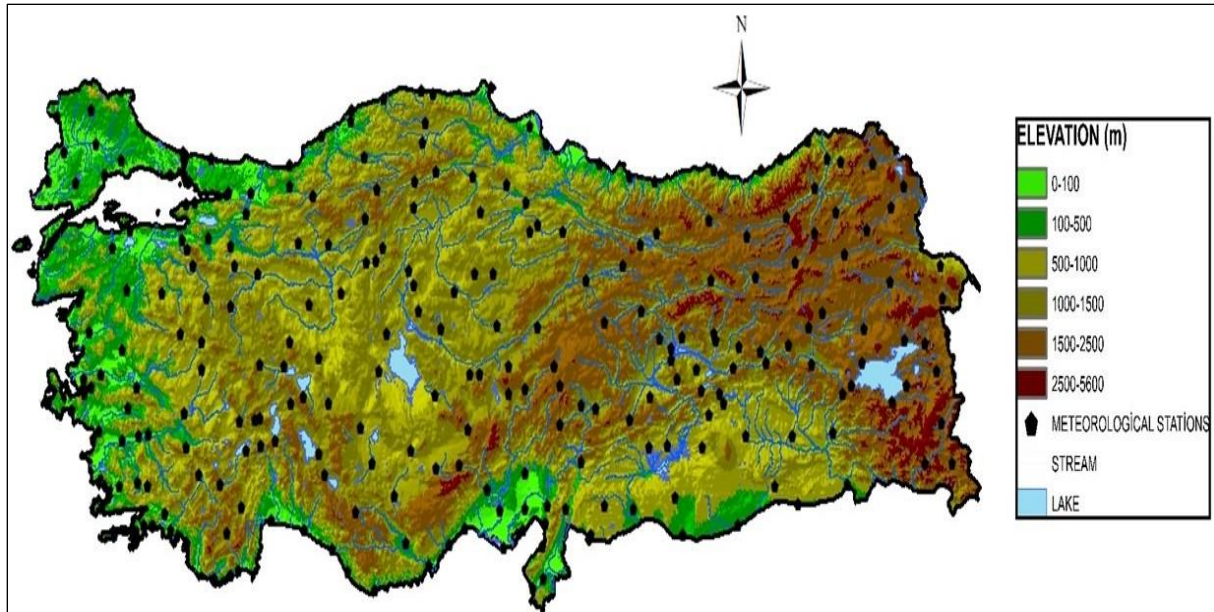
89 These studies show that reanalysis datasets such as CFSR are of sufficient quality and
90 resolution to be used as inputs in basin modelling studies. In addition, this dataset can be an important
91 alternative for overcoming problems encountered in obtaining meteorological observation data. The
92 purpose of this study is to investigate the availability and use of the CFSR reanalysis dataset for the
93 calculation of PET using the FAO56-Penman method in Turkey.

94 **2. Material and Methods**

95 **2.1. Study area and meteorological data**

96 Turkey is located between 36° - 42° N and 26° - 45° E. The total area is 779,452 square
97 kilometers and the average altitude is 1141 meters. Turkey's climate is located between the temperate
98 and sub-tropical zones. In coastal areas, milder climate features are observed with the effect of the
99 seas. The mountains of North Anatolia and the mountains of Taurus prevent the effects of the sea from
100 entering the interior parts and therefore the continental climatic characteristics are observed in the
101 interior parts (Katipoglu et al. 2021).

102 In this study, meteorological observation data from 259 stations belonging to the Turkish State
103 Meteorological Service were used for the calculation of PET. The locations of these stations are shown
104 in Figure 1 on the elevation map of Turkey.



105

106

Figure 1. Study area and location of meteorological stations

107

108

109

110

The observed potential evapotranspiration values were obtained from the "Plant Water Consumption Guide" published by State Hydraulic Works and the Directorate-General for Agricultural Research and Policy (TAGEM 2017). CFSR data set containing daily data on temperature, humidity, precipitation, wind speed and solar radiation for the years 1987 to 2017.

111 2.2. CFSR reanalysis dataset

112

113

114

115

116

117

The CFSR dataset used in this study consists of six hours of weather prediction generated by the US National Weather Service. The CFSR reanalysis dataset contains the maximum and minimum temperatures ($^{\circ}\text{C}$), precipitation (mm), wind velocity (m s^{-1}), humidity (%), and solar radiation (MJ m^{-2}) from any location in the world (Dile and Srinivasan 2014; Irvem and Ozbuldu 2019). The spatial and temporal resolution of the CFSR is 0.35° (nearly 38 km) and 6 hours, respectively. CFSR datasets for Turkey (1987–2017) were obtained via the internet (<https://rda.ucar.edu/>).

118 2.3. FAO56-PM method

119

120

121

122

Penman (1948) developed an evaporation formula for open water surface based on climatic data. Monteith (1976) developed this formula by adding aerodynamics and surface strength factors. Daily potential evapotranspiration (PET, mm day^{-1}) estimated by Penman-Monteith equation (PM) is calculated by given Eq.1.;

$$123 \quad PET = \frac{0.408 \Delta (R_n - G) + \frac{900 \gamma}{T + 273} u_2 (e_s - e_a)}{\Delta + \gamma (1 + 0.34 u_2)} \quad (1)$$

124 where; Δ is the slope of the relationship between saturation vapor pressure and mean daily air
 125 temperature ($\text{kPa } ^\circ\text{C}^{-1}$), R_n is the net radiation at the crop surface ($\text{MJ m}^{-2} \text{ day}^{-1}$), G is the soil heat flux
 126 density ($\text{MJ m}^{-2} \text{ day}^{-1}$), γ is the psychrometric constant which depends on the altitude of each location
 127 ($\text{kPa } ^\circ\text{C}^{-1}$), T is the mean daily air temperature ($^\circ\text{C}$), u_2 is the wind speed at 2 m height (m s^{-1}); e_s is the
 128 saturation vapor pressure (kPa); e_a is the actual vapor pressure (kPa).

129 **2.4. Inverse Distance Weighting (IDW) method**

130 In this study, the IDW interpolation method was used to produce a spatial distribution of the
 131 PET values. IDW is the most widely used non-geostatistical interpolation method, requiring minimal
 132 operator parameters. It can particularly be used where the data set is deficient and other techniques are
 133 affected by errors. The IDW method is a local intermediate value estimation method because it
 134 generates estimates from neighbouring points. The assigned weights at each nearby point are the
 135 opposite of its distance from the cell is estimated. The IDW method estimates unknown points using
 136 point-to-point distances in the weight calculation. The calculation formula of IDW was given in Eq.2.
 137 (Salekin et al. 2018).

$$138 \quad Z_j = \frac{\sum_{i=1}^n \frac{Z_i}{(h_{ijk} + \delta)^\beta}}{\sum_{i=1}^n \frac{1}{(h_{ijk} + \delta)^\beta}} \quad (2)$$

139 where Z_j is the unsampled location value, Z_i is the known cell's value, β is the weight, and δ is
 140 the parameter. The separation distance h_{ijk} is measured by a three-dimensional Euclidian distance. h_{ijk}
 141 is calculated by the Eq.3. (Salekin et al. 2018).

$$142 \quad h_{ijk} = \sqrt{(\Delta x)^2 + (\Delta y)^2 + (\Delta z)^2} \quad (3)$$

143 where Δx and Δy are the distances between the unknown and known point according to the
 144 reference axes, respectively, and Δz refer to the height as the third point of measure.

145 **2.5. Evaluation criteria**

146 The four statistical methods were used to assess the PET estimates from the CFSA dataset
 147 against the PET calculated using meteorological station data. These are coefficient of determination
 148 (R^2), root-mean-square error (RMSE), PBias (percent bias), and the performance index (C').

149 R^2 shows to what extent the PET estimates calculated with the CFSR dataset are similar to the
 150 PET values calculated with the observation data. R^2 varies between 0 and 1, higher values indicate less
 151 error variation. Generally, values above 0.50 are considered acceptable (Moriassi et al. 2007) and
 152 calculated based on Eq 4.;

$$153 \quad R^2 = \left(\frac{n \sum(O_i M_i) - (\sum O_i)(\sum M_i)}{\sqrt{(n(\sum O_i^2) - (\sum O_i)^2)(n(\sum M_i^2) - (\sum M_i)^2)}} \right)^2 \quad (4)$$

154 The value of RMSE should always be positive and it is desired to be close to zero. This
 155 indicates that the lower the value, the better the model will perform. RMSE provides performance
 156 information for correlations by comparing the difference between model results and observed values
 157 (Piñeiro et al. 2008). RMSE is calculated by Eq.5.

$$158 \quad RMSE = \sqrt{\frac{1}{n} \sum (Predict_i - Obs_i)^2} \quad (5)$$

159 PBias is used to determine how far the model predicted values are in the negative or positive
 160 direction from the observed values. Whereas positive values indicate that the observed values are
 161 higher than the simulated values, negative values indicate the opposite situation (Gupta et al. 1999).
 162 PBias is determined by Eq.6.

$$163 \quad PBias = 100 (\sum Obs_i - Predict_i / \sum Obs_i) \quad (6)$$

164 The Willmott index of agreement (d) shows the degree of fit between observed and predicted
 165 measurements between 0 and 1. The closer the result is to 1, the better the model performance is
 166 determined (Willmott 1981; Tran et al. 2020). It is calculated by Eq. 7.

$$167 \quad d = \frac{\sum (Obs_i - Predict_i)^2}{\sum ([Predict_i - Obs_{mean}] + [Obs_i - Obs_{mean}])^2} \quad (7)$$

168 The performance index (C') was calculated by combining accuracy and precision criteria into
 169 the relationship between the model and the predictive data. The Pearson linear correlation coefficient,
 170 which measures the degree and direction of distribution among variables, was used as a precision
 171 criterion. The Willmott's index of agreement was chosen as an accuracy criterion because it measures
 172 the degree of fit between the predicted and observed data. The performance index of the model was
 173 computed by Eq. 8 and evaluated using Table 1 (Santos et al. 2020).

$$174 \quad C' = \text{Correlation Coefficient (CC)} * \text{Willmott's index of agreement}(d) \quad (8)$$

175 **Table 1.** Model performance evaluation table (Moriiasi et al. 2007; Santos et al. 2020).

Classification	C'	PBias
Very Good	0.75 - 1.00	$< \pm 10$
Good	0.65 - 0.75	$\pm 10 - \pm 15$
Satisfactory	0.60 - 0.65	$\pm 15 - \pm 25$
Unsatisfactory	< 0.50	$> \pm 25$

176 3. Results and Discussion

177 Using meteorological data from the CFSR data set, the average seasonal and annual potential
 178 evapotranspiration amounts for each observation station for 1987-2017 were estimated. The PET
 179 estimates were compared with the PET computed using ground observation data. The accuracy and
 180 usability of the CFSR reanalysis dataset were evaluated through statistical analysis. The results of that
 181 analysis are presented in Table 2. In addition, maps were generated using IDW interpolation
 182 techniques to show area distributions of PET results for the different seasons and the long-term annual
 183 mean.

184 3.1. Results of PET estimation for the winter

185 The PET prediction results using the CFSR dataset for the winter season (December, January,
 186 February) were compared with the PET results obtained from the observed data. The obtained values
 187 for the stations were used to generate PET maps of Turkey.

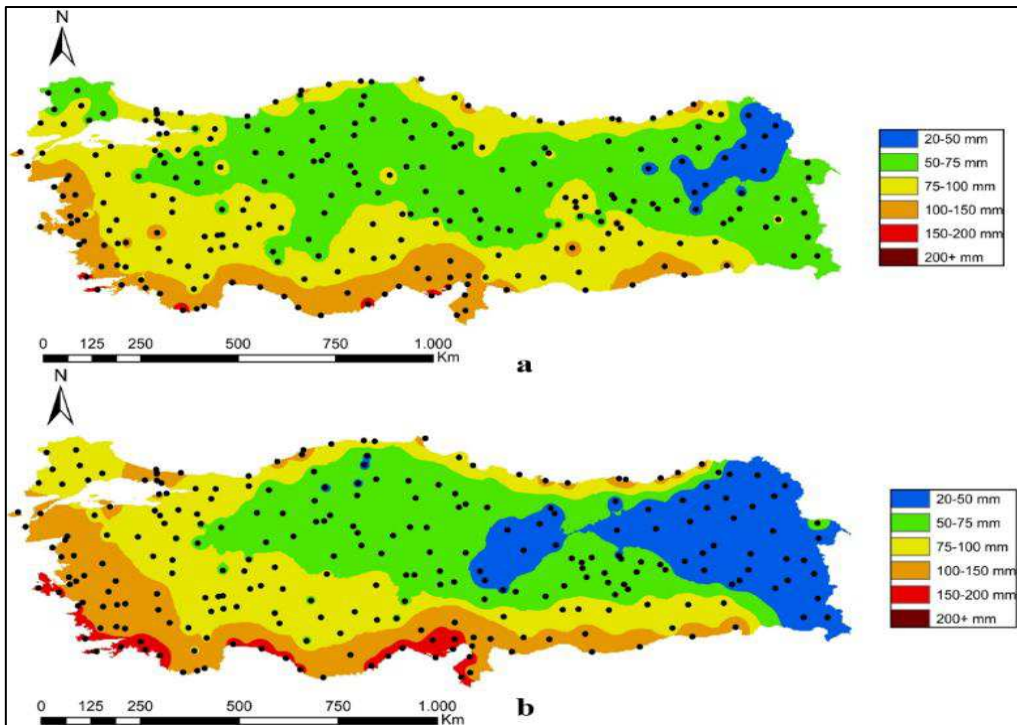
188 **Table 2.** Results of the statistical analysis

	<i>Winter(DJF)</i>	<i>Spring(MAM)</i>	<i>Summer(JJA)</i>	<i>Autumn(SON)</i>	<i>Annual</i>
R ²	0.73	0.67	0.67	0.79	0.68
RMSE	22.27	33.85	103.10	32.47	208.37
PBias	-3.77	-6.24	-16.94	-12.10	-15.27
d	0.89	0.85	0.70	0.85	0.74
C'	0.76	0.70	0.57	0.75	0.60

189

190 PET values were classified into 6 categories between 20 and 200 mm, as shown in Figure 2.
 191 When the map is examined, it is seen that CFSR has higher estimates in the southern and western
 192 regions, but lower forecasts at eastern stations. It can be explained that the CFSR reanalysis dataset
 193 has relatively high data on temperature and solar radiation in those regions, unlike the eastern region.

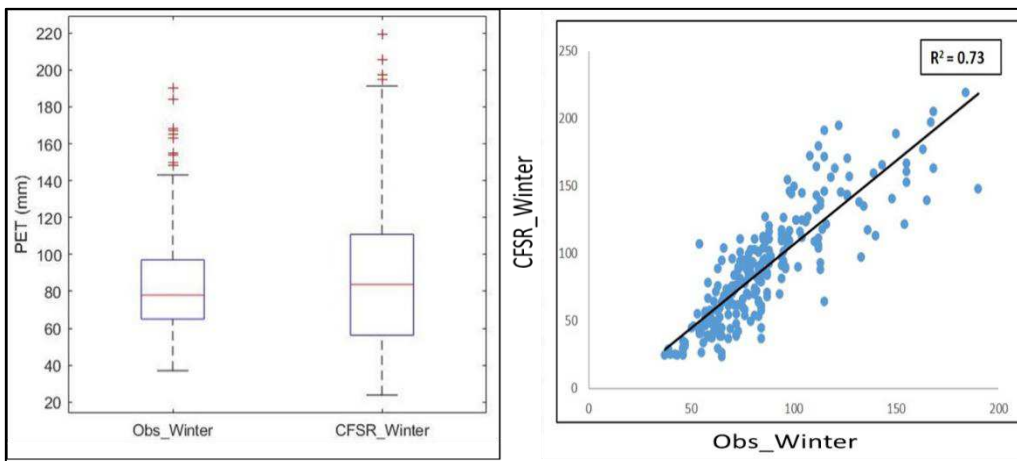
194 Bhattacharya et al. (2020) reported similar results in their study in India. They explained that
 195 the CFSR has a tendency to predict higher temperatures (>2°C) in the southwest in winter and colder
 196 temperatures in the northeast. Station estimates were compared using the calculated PBias value (-
 197 3.77) and PET calculated using CFSR data was determined to be relatively high. However, according
 198 to Table 2, these estimates are in acceptable ranges (very well <±10).



199

200

Figure 2. Average long-term PET map for the winter season a) observation b) CFSR



201

202

Figure 3. Boxplot and scatter plot of the CFSR data set for the winter season.

203

204

205

206

207

208

209

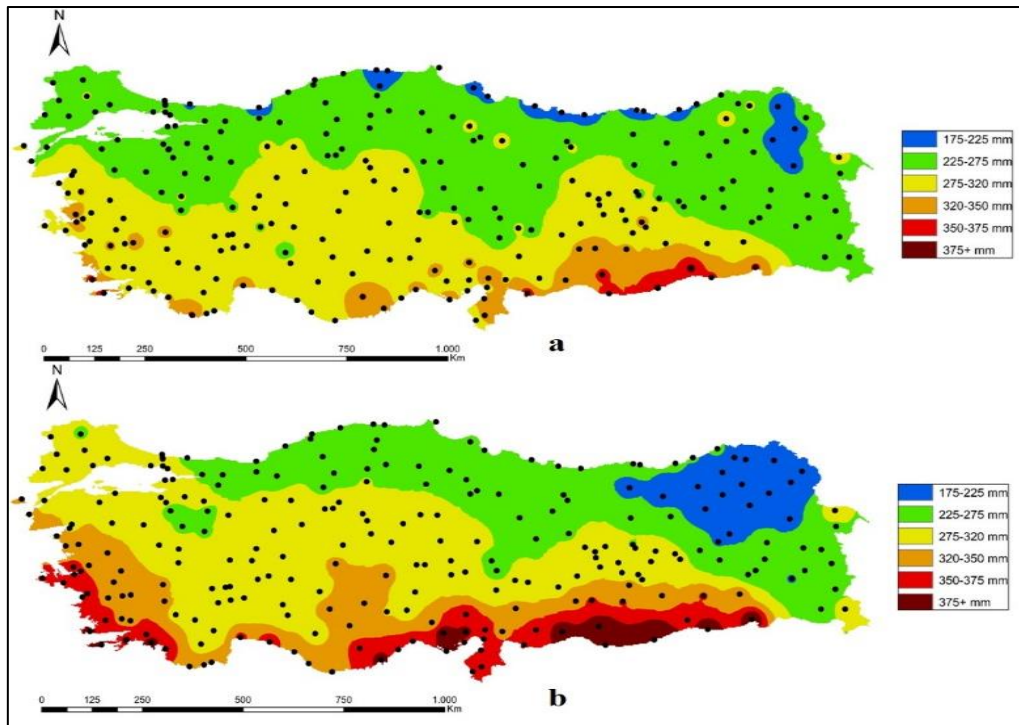
The variation of the winter season between CFSR re-analysis and observation data sets is shown in the boxplot graph in Figure 3. When we examine the two data sets, the difference between the medians is very small and the interquartile range is similar. This shows that most of the predictions made for the winter season of the CFSR data set are in line with the observation data. The R^2 value calculated 0.73 as seen in the scatter plot in Figure 3. This shows that the CFSR re-analysis dataset has a good correlation with the observation data. R^2 values between 0.50-0.99 are considered good estimates for hydrological studies (Alfaro et al. 2020). The RMSE value, which shows the amount of

210 error in the data set, was 22.77 mm season⁻¹, and the C'performance index, which shows the success
211 of the predictions, was 0.76. According to the performance evaluation, it has been observed that the C'
212 value of the CFSR estimates is quite good (>0.75). These results yielded similar results to the study
213 conducted by Tian et al. (2014), and it was observed that the predictions made with the CFSR data set
214 can be used safely for regions with missing PET estimates in the winter season.

215 **3.2. Evaluating PET estimates for the spring**

216 The spatial distributions of the estimated and observed PET results over Turkey for the spring
217 season (March, April, May) are given in Figure 4. It was seen that there were relatively similar results
218 for the stations, especially in the inner regions. However, as in the winter forecasts, the CFSR has
219 shown overestimates in the southern and western regions, and underestimates at stations in the
220 northeast region. It is seen that the CFSR reanalysis data set tends to predict PET higher than the
221 observation data. This is likely due to the CFSR having overestimations for the stations having a
222 relatively higher temperature, solar radiation, and wind speed than others (Paredes et al. 2017).

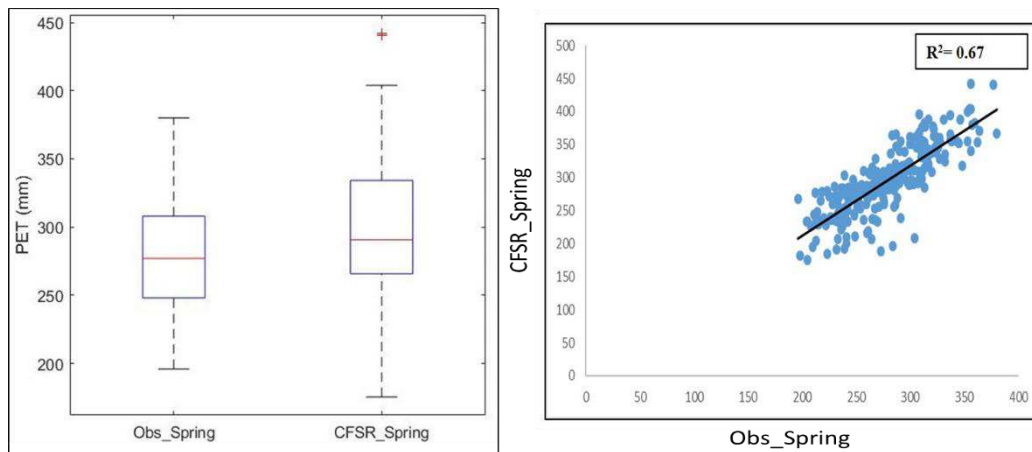
223 The R² value was found 0.67 as seen in the scatter plot in Figure 5. This shows that the CFSR
224 re-analysis dataset has a good correlation with the observed data. The RMSE value was 33.85 mm
225 season⁻¹, and the C'performance index, was 0.70. When the station estimates are compared, the
226 calculated PBias (-6.24) value indicates that the CFSR re-analysis made relatively overestimates, but
227 according to Table 2, it is in acceptable ranges (very good $\leq \pm 10$). According to these performance
228 evaluations, it was concluded that estimations of PET using the CFSR data set are also good for spring
229 seasons.



230

231

Figure 4. Average long-term PET map for the spring season a) observation b) CFSR



232

233

Figure 5. Boxplot and scatter plot of the CFSR data set for the spring season.

234 3.3. Evaluating PET estimates for the summer season

235

236

237

238

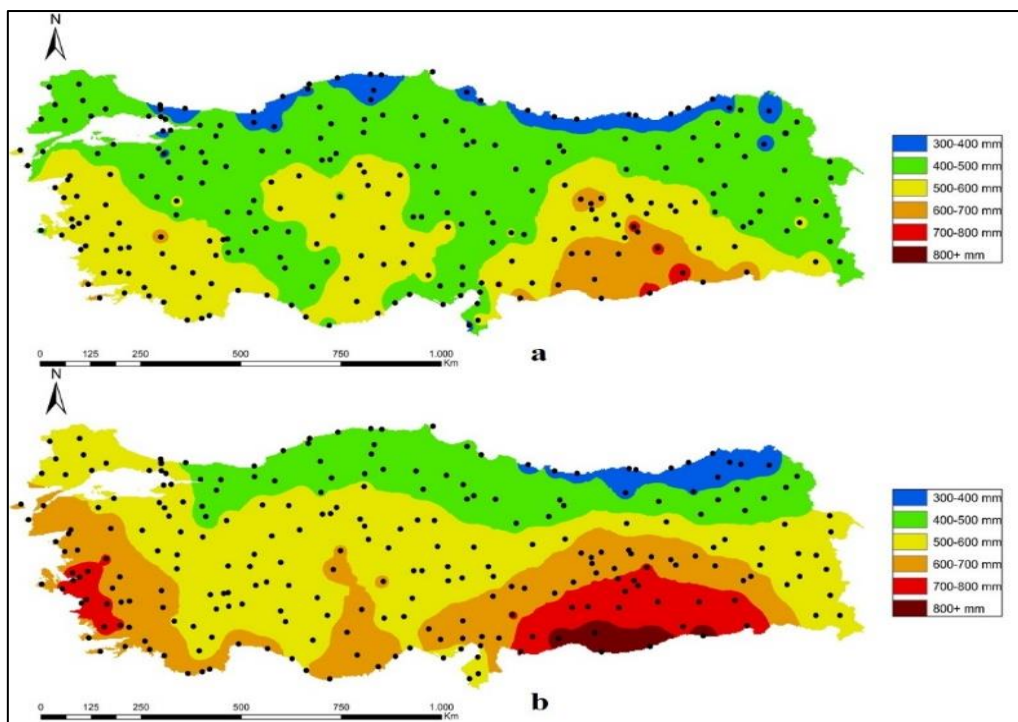
239

240

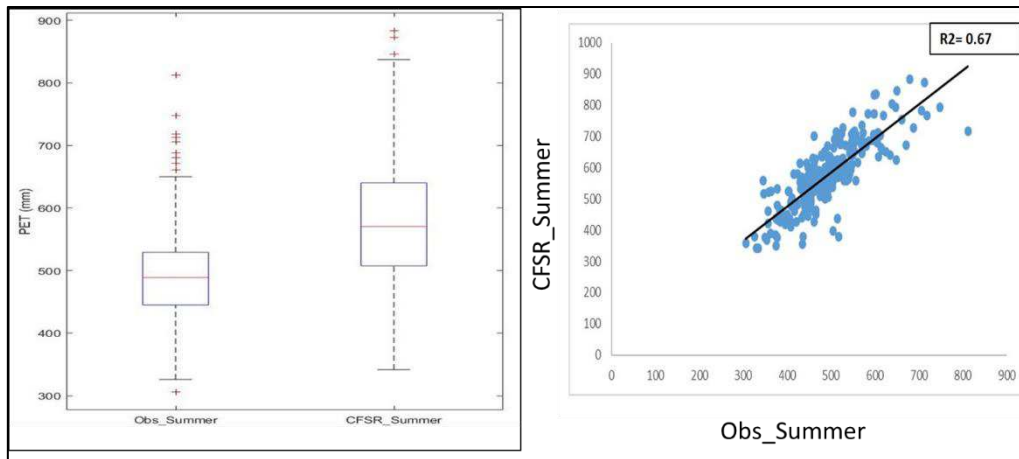
When the predictions made by the CFSR for the summer season (June, July, August) are compared with the observation data, the differences between the results are higher than in other seasons as seen in Figure 6. The reason for this thought is that temperature and solar radiation increase considerably in the summer months and the CFSR reanalysis data set cannot accurately predict these changes. CFSR was generally overestimated from the observation data where differences were higher between winter and summer seasons, especially in the southeastern and western regions.

241 PBias value was calculated -16.94 for the summer season. It shows that the CFSR re-analysis
242 made higher estimates in summer than winter and spring, but estimated PET for the summer is still in
243 acceptable (± 25) ranges.

244 Although PET estimates are acceptable in terms of R^2 (0.67), the RMSE had the highest error
245 (RMSE=103.10 mm season⁻¹), and the C' performance index is 0.57. According to these performance
246 evaluations, the C' value of the CFSR estimates is not acceptable (<0.60). The reason why the PET
247 prediction of the CFSR re-analysis dataset underperforms in the summer is due to the decrease in solar
248 radiation and temperature prediction capabilities. The reason can be explained that more convective
249 warming occurs in summer compared to other seasons. This type of convection may cause the
250 formation of different weather conditions on a small scale that CFSR cannot predict due to its coarse
251 resolution (Tian et al., 2014). Using the CFSR data set directly on models for the summer months will
252 result in unsuccessful simulation results. For this reason, preliminary procedures that will reduce this
253 dataset to a regional scale should be applied and re-evaluated before using it.



254
255 **Figure 6.** Average long-term PET map for the summer season a) observation b) CFSR



256

257

Figure 7. Boxplot and scatter plot of the CFSR data set for the summer season.

258 **3.4. Evaluating PET estimates for the autumn**

259

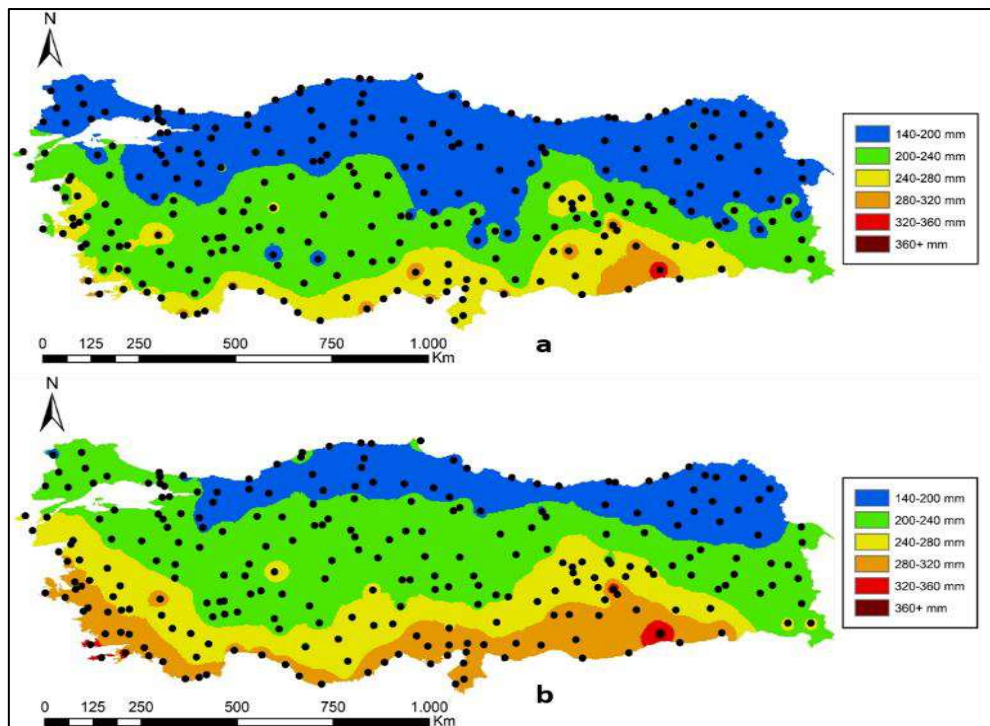
The predictions made by the CFSR for the autumn season (September, October, November)

260

PET estimated higher than observation data as seen in Figure 8. The PBias was found -12.10. This

261

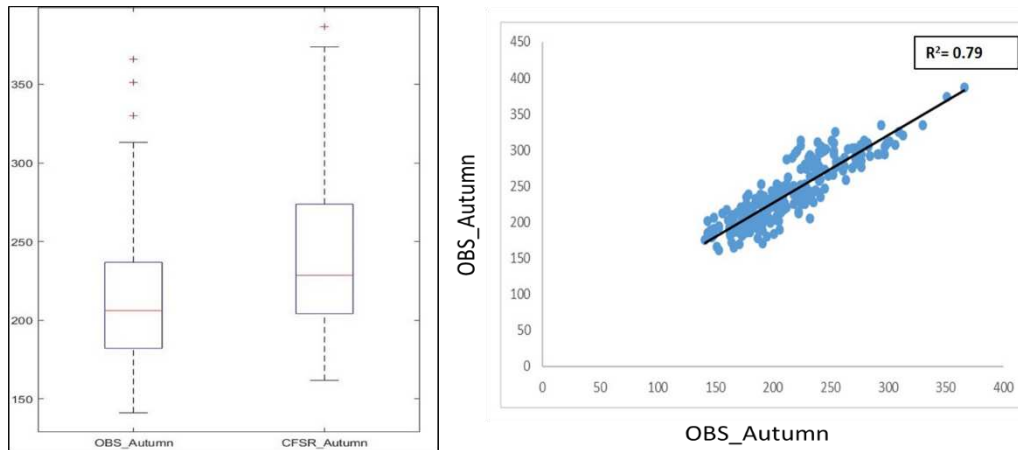
shows that the CFSR re-analysis estimates PET is good ($< \pm 15$).



262

263

Figure 8. Average long-term PET map for the autumn season a) observation b) CFSR



264

265

Figure 9. Boxplot and scatter plot of the CFSR data set for the spring season.

266

267

268

269

270

271

272

273

The boxplot graph for the autumn season between the CFSR reanalysis and observation data sets is given in Figure 9. When comparing the situation between quarters, it is seen that the higher estimates of CFSR for the autumn season are more intense. Because of the R^2 value found 0.79, PET estimates of CFSR data are good for the autumn season. This shows that the CFSR re-analysis dataset has a good correlation with the observed data. The RMSE value and C' performance index were calculated $32.47 \text{ mm season}^{-1}$, and 0.75 respectively. According to the performance evaluation, the C' value of the CFSR estimates is quite good (>0.75). These results show that the CFSR estimates of PET for the autumn season can be used safely.

274

3.5. Evaluating long-term average annual pet estimates

275

276

277

278

279

280

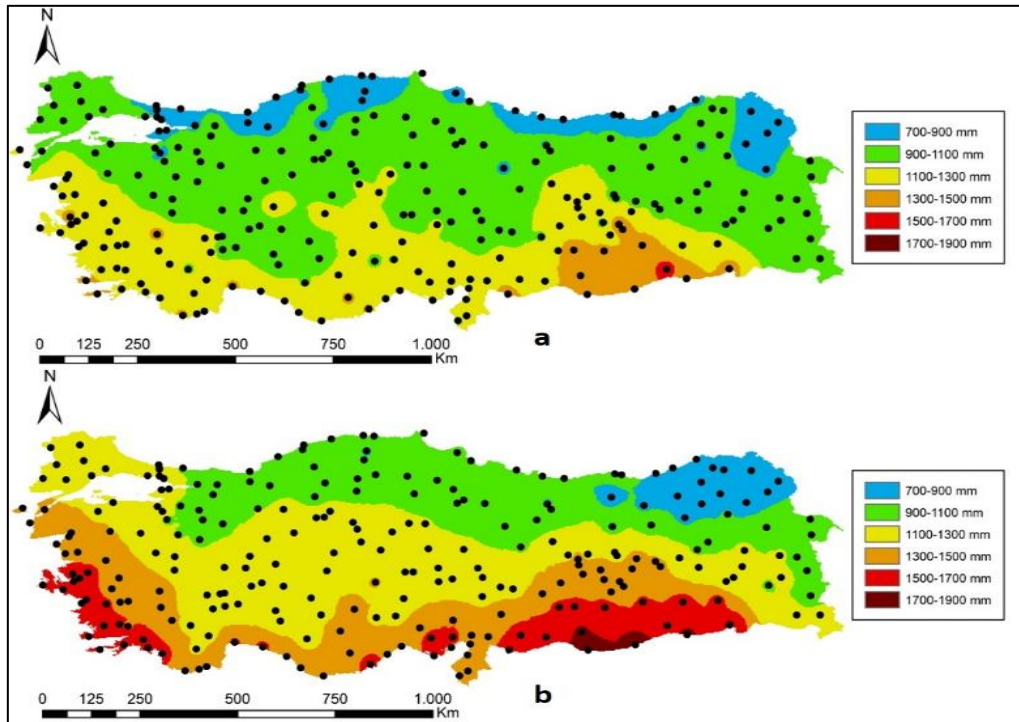
281

282

283

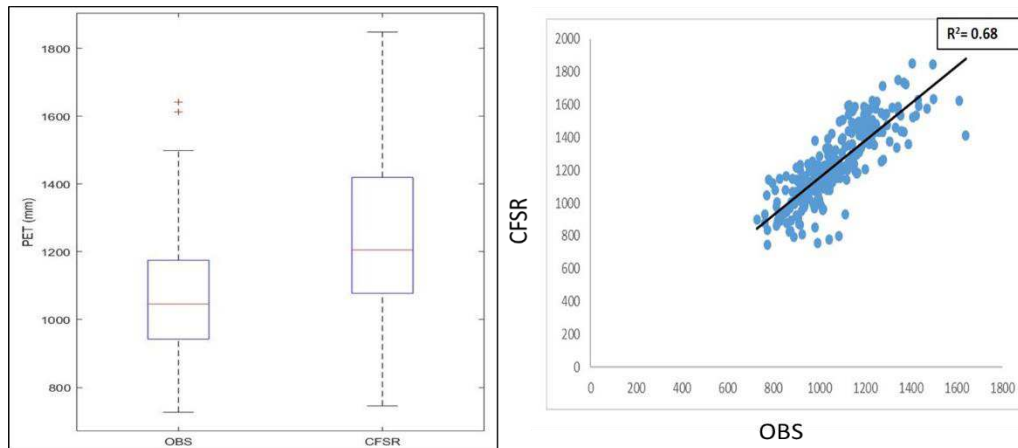
The long-term annual average PET estimations using the CFSR data set and observed data for the years 1987-2017 are shown in Figure 10. PET was estimated between 1300-1900 mm/year for Southern and Western regions in Turkey. In this region, PET was calculated between 1100-1700 mm using data from meteorological observation stations. In contrast, estimated and observed PET were found lower in the northern and eastern regions of Turkey. Estimated PET using CFSR was between 700-1100 mm year^{-1} in the northern and eastern regions and 900-1300 mm in inland regions. These estimates are very close to the observation data as can be seen in Figure 10. In the study conducted in China, while PET estimates for the south and west regions were high, it was observed that the PET estimates for other regions were similar to the station results (Tian et al. 2018).

284 When the station estimates are compared, the calculated Pbias (-15.27) value shows that the
285 CFSR reanalysis estimates are acceptable ($< \pm 25$). The negative result of the PBias indicates that the
286 long-year average CFSR PET estimates are higher than the observation calculations.



287
288 **Figure 10.** Average long-term annual PET map a) observation b) CFSR and

289 Calculated and estimated PET distributions using the average long annual data are shown in
290 Figure 11 with the boxplot. When comparing the situation between quarters, it is seen that the higher
291 estimates are more intense. It has been observed that the minimum values are close to each other, but
292 in the difference between the maximum values, it is seen that the CFSR tends to overestimate PET
293 annually from the observation data. The R^2 value (0.68) shows that the annual PET estimates are
294 acceptable and have a good correlation with observation data. The RMSE value showing the amount
295 of error in the data set was calculated as $208.37 \text{ mm year}^{-1}$. The C' performance index, which shows
296 the success of the predictions, was obtained as 0.60. According to the performance evaluation, it has
297 been observed that the C' value of the CFSR estimates is acceptable (> 0.60). Alfaro et al. (2020)
298 calculated the C' performance index of the CFSR reanalysis data set as 0.72 in their study conducted in
299 Brazil and explained that the prediction performance was acceptable similar to our study results.



300

301 **Figure 11.** Boxplot and scatter plot of long-term average annual CFSR re-analysis data set

302 **4. Conclusion**

303 PET is a very important parameter for hydrological, meteorological, and agricultural studies.
 304 However, it is very difficult to obtain the meteorological data for calculation or estimation of this
 305 parameter in developing countries for the required regions. In this study, PET was estimated by the
 306 FAO56-PM method using observed and CFSR data set for Turkey. Accuracy of seasonal and annual
 307 estimations was statistically evaluated by comparing calculated PET. Data from 259 stations covers
 308 the period from 1987 to 2017 used to calculate PET.

309 As a result of the evaluations, the periods in which the prediction performance of the CFSR
 310 reanalysis data set was the highest were determined as Winter ($C' = 0.76$ and $PBias = -3.77$) and
 311 Autumn ($C' = 0.75$ and $PBias = -12.10$) seasons. Also, the lowest RMSE values were calculated (22.27
 312 and 32.47) in these two seasons. The worst performance was seen for the Summer season ($C' = 0.57$
 313 and $PBias = -16.94$). The reason for this, the increase in solar radiation and temperature values during
 314 the summer months cannot be estimated by the CFSR accurately as mentioned by Tian et al. (2014). In
 315 terms of annual performance, it has been calculated as $C' = 0.60$ and $PBias = -15.27$. These results
 316 show that the PET prediction ability of the CFSR re-analysis dataset is relatively good for the study
 317 area.

318 $PBias$ value was calculated as negative in annual and seasonal evaluations. Especially in the
 319 southern and western regions, it has been observed that CFSR tends to overestimate the observation

320 data. Similar results have been observed in studies conducted by Bhattacharya et al. (2020) and Tian et
321 al. (2017).

322 Therefore, when the CFSR reanalysis data set is evaluated in general, it can be seen as a good
323 potential data source. However, it is recommended to evaluate the data with observation data before
324 being used especially in summer seasons and to be used after regionalization with downscaling
325 methods before being used in models.

326 **Author information**

327 **Affiliations**

328 Department of Biosystems Engineering, Faculty of Agriculture, Hatay Mustafa Kemal University,
329 31040, Antakya, Hatay, Turkey.

330 Ahmet Irvem, Mustafa Ozbuldu

331 **Corresponding author**

332 Correspondence to Ahmet Irvem

333 **Author contributions**

334 All authors contributed to the study conception and design. Material preparation, data collection and
335 analysis were performed by Ahmet Irvem and Mustafa Ozbuldu.

336 **Funding**

337 This research received no specific grant from any funding agency in the public, commercial, or not-
338 for-profit sectors.

339 **Data availability**

340 The data that support the findings of this study will be made available from the corresponding author
341 on reasonable request.

342 **Code availability**

343 Not applicable.

344 **Ethics declarations**

345 **Ethics approval:**

346 The authors have agreed for authorship, read and approved the manuscript, and given consent for
347 submission and subsequent publication of the manuscript.

348 **Consent to participate**

349 All authors consent to participate of the present study.

350 **Consent for publication**

351 All authors consent to participate of the present study.

352 **Conflict of interest**

353 The authors declare no competing interests.

354 **References**

355 Alemayehu T, van Griensven A, Bauwens W (2016) Evaluating CFSR and WATCH data as input to
356 SWAT for the estimation of the potential evapotranspiration in a data-scarce Eastern-African
357 catchment. *J Hydrol Eng* 21(3):1–16. [https://doi.org/10.1061/\(ASCE\)HE.1943-5584.0001305](https://doi.org/10.1061/(ASCE)HE.1943-5584.0001305)

358 Alfaro MDM, Lopes I, Montenegro AAA, Leal BG (2020) CFSR- NCEP performance for weather
359 data forecasting in the Pernambuco Semiarid, Brazil. *DYNA* 87(215):204-213.
360 <http://doi.org/10.15446/dyna.v87n215.89952>

361 Allen RG, Pereira SL, Raes D, Smith M (1998) Crop evapotranspiration. Guidelines for computing
362 crop water requirements. FAO Irrigation and Drainage Paper 56, Rome, pp 300

363 Anderson M, Diak G, Gao F, Knipper K, Hain C, Eichelmann E, Hemes K, Baldocchi D, Kustas W,
364 Yang YJRS (2019) Impact of insolation data source on remote sensing retrievals of evapotranspiration
365 over the California Delta. *Remote Sens* 11:216. <https://doi.org/10.3390/rs11030216>

366 Auerbach DA, Easton ZM, Walter MT, Flecker AS, Fuka DR (2016) Evaluating weather observations
367 and the Climate Forecast System Reanalysis as inputs for hydrologic modelling in the tropics. *Hydrol*
368 *Process* 30(19):3466–3477. <https://doi.org/10.1002/hyp.10860>

369 Bandyopadhyay A, Bhadra A, Swarnakar RK, Raghuwanshi NS, Singh R (2012) Estimation of
370 reference evapotranspiration using a user-friendly decision support system: DSS_ET. *Agr Forest*
371 *Meteorol* 154:19–29. <https://doi.org/10.1016/j.agrformet.2011.10.013>

372 Bromwich DH, Wang SH (2005) Evaluation of the NCEP-NCAR and ECMWF 15- and 40-yr
373 reanalyses using rawinsonde data from two independent Arctic field experiments. *Mon Weather Rev*
374 133:3562–3578. <https://doi.org/10.1175/MWR3043.1>

375 Conceição MAF (2002) Reference evapotranspiration based on Class A-pan evaporation. *Sci Agric*.
376 59(3):417-420. <https://doi.org/10.1590/S0103-90162002000300001>

377 Dee DP, Uppala S, Simmons A, Berrisford P, Poli P, Kobayashi S, Andrae U, Balmaseda M, Balsamo
378 G, Bauer P (2011) The ERA-Interim reanalysis: Configuration and performance of the data
379 assimilation system. *Q J Roy Meteor Soc* 137:553–597. <https://doi.org/10.1002/qj.828>

380 Dile YT, Srinivasan R (2014) Evaluation of CFSR Climate Data for Hydrologic Prediction in Data-
381 Scarce Watersheds: An Application in the Blue Nile River Basin. *J Am Water Resour As* 50:1226–
382 1241. <https://doi.org/10.1111/jawr.12182>

383 Ebita A, Kobayashi S, Ota Y, Moriya M, Kumabe R, Onogi K, Harada Y, Yasui S, Miyaoka K,
384 Takahashi K, Kamahori H, Kobayashi C, Endo H, Soma M, Oikawa Y, Ishimizu T (2011) The
385 Japanese 55-year Reanalysis “JRA-55”: An interim report. *SOLA* 7:149–152.
386 <https://doi.org/10.2151/sola.2011-038>

387 Fuka DR, Walter MT, MacAlister C, Degaetano AT, Steenhuis TS, Easton ZM (2013) Using the
388 Climate Forecast System Reanalysis as weather input data for watershed models. *Hydrol Process*
389 28:5613–5623. <https://doi.org/10.1002/hyp.10073>

390 Gebler S, Hendricks Franssen HJ, Putz T, Post H, Schmidt M, Vereecken H (2015) Actual
391 evapotranspiration and precipitation measured by lysimeters: A comparison with eddy covariance and
392 tipping bucket. *Hydrol Earth Syst Sc* 19:2145–2161. <https://doi.org/10.5194/hess-19-2145-2015>

393 Gupta HV, Sorooshian S, Yapo PO (1999) Status of automatic calibration for hydrologic models:
394 comparison with multilevel expert calibration. *J Hydrol Eng* 4(2):135–143.
395 [https://doi.org/10.1061/\(ASCE\)1084-0699\(1999\)4:2\(135\)](https://doi.org/10.1061/(ASCE)1084-0699(1999)4:2(135))

396 Irvem A, Ozbuldu M 2019 Evaluation of Satellite and Reanalysis Precipitation Products Using GIS for
397 All Basins in Turkey. *Adv Meteorol* 2019(4820136):1–11. <https://doi.org/10.1155/2019/4820136>

398 Kalnay E, Kanamitsu M, Kistler R, Collins W, Deaven D, Gandin L, Iredell M, Saha S, White G,
399 Woollen J, Zhu Y, Chelliah M, Ebisuzaki W, Higgins W, Janowiak J, Mo KC, Ropelewski C, Wang J,
400 Leetmaa A, Reynolds R, Jenne R, Joseph D (1996) The NCEP NCAR 40-year reanalysis project. *B*
401 *Am Meteorol Soc* 77:437–472. <https://doi.org/10.1175/1520-0477>

402 Kanamitsu M, Ebisuzaki W, Woollen J, Yang SK, Hnilo JJ, Fiorino M, Potter GL (2002) NCEP–DOE
403 amip-ii reanalysis (r-2). *B Am Meteorol Soc* 83(11):1631–1644. <https://doi.org/10.1175/BAMS-83->
404 [11-1631](https://doi.org/10.1175/BAMS-83-11-1631)

405 Katipoglu OM, Acar R, Senocak S (2021) Spatio-temporal analysis of meteorological and
406 hydrological droughts in the Euphrates Basin, Turkey. *Water Supp*, ws2021019.
407 <https://doi.org/10.2166/ws.2021.019>

408 Kite GW, Droogers P (2000) Comparing evapotranspiration estimates from satellites, hydrological
409 models and field data. *J Hydrol* 229:3–18. [https://doi.org/10.1016/S0022-1694\(99\)00193-6](https://doi.org/10.1016/S0022-1694(99)00193-6)

410 Lang D, Zheng J, Shi J, Liao F, Ma X, Wang W, Chen X, Zhang M (2017) A comparative study of
411 potential evapotranspiration estimation by eight methods with FAO Penman–Monteith Method in
412 Southwestern China. *Water* 9:1–18. <https://doi.org/10.3390/w9100734>

413 Latrech B, Ghazouani H, Lasram A, M’hamdi BD, Mansour M, Boujelben A (2019) Assessment of
414 different methods for simulating actual evapotranspiration in a semi-arid environment. *Ital J*
415 *Agrometeoro* 2:21-34. <https://doi.org/10.13128/ijam-650>

416 Lauri H, Räsänen TA, Kumm M (2014) Using reanalysis and remotely sensed temperature and
417 precipitation data for hydrological modeling in monsoon climate: Mekong River case study. *J*
418 *Hydrometeorol* 15:1532–1545. <https://doi.org/10.1175/JHM-D-13-084.1>

419 Moorhead JE, Marek GW, Colaizzi PD, Gowda PH, Evett SR, Brauer DK, Marek TH, Porter DO
420 (2017) Evaluation of sensible heat flux and evapotranspiration estimates using a surface layer

421 scintillometer and a large weighing lysimeter. *Sensors* 17:2316–2350.
422 <https://doi.org/10.3390/s17102350>

423 Moriasi DN, Arnold JG, Van Liew MV, Bingner RL, Harmel RD, Veith TL (2007) Model evaluation
424 guidelines for systematic quantification of accuracy in watershed simulations. *T ASABE* 50(3):885–
425 900. <https://doi.org/10.13031/2013.23153>

426 Paredes P, Martins DS, Pereira LS, Cadima J, Pires C (2017) Accuracy of daily PM-ET_o estimations
427 with ERA-Interim reanalysis products. *Euro Water* 59:239-246.

428 Piñeiro G, Perelman S, Guerschman JP, Paruelo JM (2008) How to evaluate models: observed vs.
429 predicted or predicted vs. observed? *Ecol Model* 216(3-4):316–322.
430 <https://doi.org/10.1016/j.ecolmodel.2008.05.006>

431 Purnadurga G, Kumar TL, Rao KK, Barbosa H, Mall RK (2019) Evaluation of evapotranspiration
432 estimates from observed and reanalysis data sets over Indian region. *Int J Clim* 39(15):5791–5800.
433 <https://doi.org/10.1002/joc.6189>.

434 Rienecker MM, Suarez MJ, Gelaro R, Todling R, Bacmeister J, Liu E, Bosilovich MG, Shubert SD,
435 Takacs L, Kim GK, Bloom S, Chen J, Collins D, Conaty A, Silva AD, Gu W, Joiner J, Koster RD,
436 Luccesi R, Molod A, Owens T, Pawson S, Pegion P, Redder CR, Reichle R, Robertson FR, Ruddick
437 AG, Sienkiewicz M, Woollen J (2011) MERRA: NASA's modern-era retrospective analysis for
438 research and applications. *J Clim* 24:3624–3648. <https://doi.org/10.1175/JCLI-D-11-00015.1>

439 Saha S, Moorthi S, Pan HL, Wu X, Wang J, Nadiga S, Tripp P, Kistler R, Woollen J, Behringer D, Liu
440 H, Stokes D, Grumbine R, Gayno G, Wang J, Hou YT, Chuang HY, Juang HMH, Sela J, Iredell M,
441 Treadon R, Kleist D, van Delst P, Keyser D, Derber J, Ek M, Meng J, Wei H, Yang R, Lord S, van
442 den Dool H, Kumar A, Wang W, Long C, Chelliah M, Xue Y, Huang B, Schemm JK, Ebisuzaki W,
443 Lin R, Xie P, Chen M, Zhou S, Higgins W, Zou CZ, Liu Q, Chen Y, Han Y, Cucurull L, Reynolds
444 RW, Rutledge G, Goldberg M (2010) The NCEP Climate Forecast System Reanalysis. *B Am
445 Meteorol Soc* 91:1015–1058. <https://doi.org/10.1175/2010BAMS3001.1>

446 Salekin S, Burgess J, Morgenroth J, Mason E, Meason D (2018) A comparative study of three non-
447 geostatistical methods for optimising digital elevation model interpolation. *ISPRS Int Geo-Inf*
448 7(8):300. <https://doi.org/10.3390/ijgi7080300>

449 Santos JFS, Leite DC, Severo FAS, Naval LP (2020) Validating the Mark-HadGEM2-ES and Mark-
450 MIROC5 climate models to simulate rainfall in the last agricultural frontier of the Brazilian North and
451 North-East Savannah. *Adv Res* 21(8):43-54. <https://doi.org/10.9734/air/2020/v21i830225>

452 Sentelhas PC, Gillespie TJ, Santos EA (2010) Evaluation of FAO Penman-Monteith and alternative
453 methods for estimating reference evapotranspiration with missing data in Southern Ontario, Canada.
454 *Agr Water Manage* 97:635-644. <https://doi.org/10.1016/j.agwat.2009.12.001>

455 Seong C, Sridhar V, Billah MM (2018) Implications of potential evapotranspiration methods for
456 streamflow estimations under changing climatic conditions. *Int J Climatol* 38 (2):896–914.
457 <https://doi.org/10.1002/joc.5218>

458 Shi TT, Guan DX, Wu JB, Wang AZ, Jin CJ, Han SJ (2008) Comparison of methods for estimating
459 evapotranspiration rate of dry forest canopy: Eddy covariance, Bowen ratio energy balance, and
460 Penman-Monteith equation. *J Geophys Res* 113(D19):D19116. <https://doi.org/10.1029/2008JD010174>

461 Srivastava PK, Han D, Ramirez MAR, Islam T (2013) Comparative assessment of evapotranspiration
462 derived from NCEP and ECMWF global datasets through Weather Research and Forecasting model.
463 *Atmos Sci Lett* 14:118–125. <https://doi.org/10.1002/asl2.427>

464 Sun G, Noormets A, Chen J, McNulty SG (2008) Evapotranspiration estimates from eddy covariance
465 towers and hydrologic modeling in managed forests in Northern Wisconsin, USA. *Agr Forest*
466 *Meteorol* 148:257-267.

467 Tabari H, Grismer ME, Trajkovic S (2013) Comparative analysis of 31 reference evapotranspiration
468 methods under humid conditions. *Irrigation Sci* 31:107–117. [https://doi.org/10.1007/s00271-011-](https://doi.org/10.1007/s00271-011-0295-z)
469 [0295-z](https://doi.org/10.1007/s00271-011-0295-z)

470 TAGEM (2017) Türkiye’de sulanan bitkilerin bitki su tüketimleri.
471 <https://www.tarimorman.gov.tr/TAGEM/Belgeler/yayin/Tu%CC%88rkiyede%20Sulanan%20Bitkileri>
472 <n%20Bitki%20Su%20Tu%CC%88ketimleri.pdf>. Accessed: 16 March 2021

473 Tanguy M, Prudhomme C, Smith K, Hannaford J (2018) Historical gridded reconstruction of potential
474 evapotranspiration for the UK. *Earth Syst Sci Data* 10(2):951–968. [https://doi.org/10.5194/essd-10-](https://doi.org/10.5194/essd-10-951-2018)
475 <951-2018>

476 Tian D, Martinez CJ, Graham WD (2014) Seasonal prediction of regional reference evapotranspiration
477 based on Climate Forecast System Version 2. *J Hydrometeorol* 15:1166–1188.
478 <https://doi.org/10.1175/JHM-D-13-087.1>

479 Tian Y, Zhang K, Xu YP, Gao X, Wang J (2018) Evaluation of potential evapotranspiration based on
480 CMADS reanalysis dataset over China. *Water* 10:1126. <https://doi.org/10.3390/w10091126>

481 Tran TMA, Eitzinger J, Manschadi AM (2020) Response of maize yield under changing climate and
482 production conditions in Vietnam. *Ital J Agrometeorol*, 1: 73-84. <https://doi.org/10.13128/ijam-764>

483 Uppala SM, Kallberg PW, Simmons AJ, Andrae U, Bechtold VDC, Fiorino M, Gibson JK, Haseler J,
484 Hernandez A, Kelly GA, Li X, Onogi K, Saarinen S, Sokka N, Allan RP, Andersson E, Arpe K,
485 Balmaseda MA, Beljaars ACM, Berg LVD, Bidlot J, Bormann N, Caires S, Chevallier F, Dethof A,
486 Dragosavac M, Fisher M, Fuentes M, Hagemann S, Hólm E, Hoskins BJ, Isaksen L, Janssen PAEM,
487 Jenne R, McNally AP, Mahfouf JF, Morcrette JJ, Rayner NA, Saunders RW, Simon P, Sterl A,
488 Trenberth KE, Untch A, Vasiljevic D, Viterbo P, Woollen J (2005) The ERA-40 re-analysis. *Q J Roy*
489 *Meteor Soc* 131:2961–3012. <https://doi.org/10.1256/qj.04.176>

490 Willmott CJ (1981) On the validation of models. *Phys Geogr* 2(2):184–194.
491 <https://doi.org/10.1080/02723646.1981.10642213>

492